Pergamon

PII: S0042-6989(96)00228-3

Vision Res., Vol. 37, No. 9, pp. 1177–1191, 1997

0042-6989/97 $17.00 + 0.00

Probed-sinewave Paradigm: a Test of Models of Light-adaptation Dynamics

D. C. HOOD,*§ N. GRAHAM,* T. E. von WIEGAND,† V. M. CHASE‡

Received 25 January 1996; in revised form 24 June 1996

Studies of light adaptation have, in general, employed either aperiodic or periodic stimuli. In earlier work, models originally developed to predict the results from one tradition failed to predict results from the other but the models from the two traditions could be merged to predict phenomena from both. To further test these merged models, a paradigm combining both types of stimuli was used. The threshold for a brief flash (the probe) was measured at various phases on a background that was varied sinusoidally in time. The probe threshold depends upon the phase at which it is presented for all background frequencies used, 0–16 Hz. These threshold variations are not well described by a sinewave; the peak threshold is >180 deg out of phase with the trough threshold. Further, the positions of the peaks and troughs shift fairly abruptly at background modulations of 4–8 Hz. The difference between the peak and trough thresholds varies as a function of temporal frequency in a manner approximating the temporal contrast sensitivity function. The dc level (mean threshold) does not. The peak–trough difference dominates at low frequencies of background modulation, while the dc level dominates for higher frequencies. Existing models of light adaptation do not predict the key features of the data. © 1997 Elsevier Science Ltd. All rights reserved.

Light adaptation Computational model Flicker Incremental threshold

INTRODUCTION

The human visual system can adjust to ambient light levels over a range of 10^8 or more. Over much of this range, we remain exquisitely sensitive to small differences in ambient light and the response to any given stimulus contrast remains approximately constant (Weber's law). The processes involved in this adjustment, or adaptation, to ambient lights may occur both in the retina and at high levels. They have been extensively studied both physiologically and psychophysically. [See reviews by Hood & Finkelstein (1986) and Shapley & Enroth-Cugell (1984).] Many properties of these processes remain unknown, however. Here we are concerned with computational models of the temporal dynamics of these processes.

A computational model should be able to predict data from a wide range of experimental paradigms. Early attempts to produce models of adaptation tended to focus either on data from experiments in which the stimuli were periodic (usually sinusoidal) or from experiments in which the stimuli were aperiodic (spots and brief flashes). In 1992, Graham and Hood chose two fundamental psychophysical paradigms, one from the periodic tradition and one from the aperiodic, and showed that existing models could predict the data from one or the other paradigm but not from both.

The aperiodic paradigm chosen by Graham and Hood measures the time course of adaptation following the onset of an adapting light. The threshold for detecting a brief light is high immediately after the onset of an adapting light, but, with time decreases to a lower level (e.g. Crawford, 1947; Baker, 1949; Boynton & Kandel, 1957). A variation on this paradigm, the probe-flash paradigm, involves a wide range of changes in the adapting flash intensities (Geisler, 1978; Hood *et al.*, 1978). The probe-flash paradigm has been used to study nonlinearities associated with light adaptation and models have been developed to predict the data (e.g. Adelson, 1982; Finkelstein *et al.*, 1990; Geisler, 1978, 1979, 1981, 1983; Hayhoe *et al.*, 1987, 1992; Hayhoe, 1990; Hood, 1978; Hood *et al.*, 1979; Hood & Finkelstein, 1986; Kortum & Geisler, 1995; Mejia-Monasterio & Gaudiano, 1995; Walraven & Valeton, 1984). A particular striking feature of the data from the probe-flash paradigm is the very steep slope of

---

*Department of Psychology, Columbia University, 406 Schermerhoun Hall, 116th Street+Broadway, New York, NY 10027, U.S.A.

†Research Laboratory of Electronics, Massachusetts Institute of Technology, Cambridge, MA 02139, U.S.A.

‡Department of Psychology, University of Chicago, Chicago, IL 60637, U.S.A.

§To whom all correspondence should be addressed [*Email* don@psych.columbia.edu].

the threshold vs illuminance (tvi) curve for probes presented immediately after the onset of the background. This feature has been called the "background-onset effect".

The periodic paradigm chosen by Graham and Hood measures the temporal contrast sensitivity of the visual system at different mean ambient light levels [e.g. De Lange, 1952, 1958; Kelly, 1961; Roufs, 1972a,b; Sperling & Sondhi, 1968; see reviews by Shapley & Enroth-Cugell (1984), Watson (1986), and Graham (1989)]. Although thresholds for low temporal frequencies of modulation follow Weber's law, the thresholds for high temporal frequencies of modulation are relatively unaffected by adaptation level; that is, they show "high-frequency linearity". A variety of models have been proposed to explain the changes in the temporal contrast sensitivity function with mean luminance (e.g. Baylor *et al.*, 1974; Dodge *et al.*, 1968; Fuortes & Hodgekin, 1964; Kelly, 1961; Kelly & Wilson, 1978; Matin, 1968; Sperling & Sondhi, 1968; Tranchina *et al.*, 1984; Tranchina & Peskin, 1988; Watson, 1986).

Graham and Hood (1992) suggested that together the background-onset effect and high-frequency linearity provide a way to test existing models of light adaptation. They concluded that no existing model could predict both high-frequency linearity and the background-onset effect. Models produced by merging parts of the models from each tradition, however, could predict both phenomena. Graham and Hood (1992) did not attempt to fit these merged models to existing data quantitatively because the experimental conditions differed substantially from one study to another. More recently, von Wiegand *et al.* (1995) proposed a model that passed the test suggested by Graham and Hood (1992). This model was fitted to data collected from the same observers using both the aperiodic and periodic paradigms and a common set of stimuli. Others are developing computational models to predict data from a range of aperiodic and periodic paradigms (e.g. Wilson, 1995).

These computational models need further testing. In the present study, we explore a paradigm that combines periodic and aperiodic stimuli. This paradigm, called here the "probed-sinewave paradigm" was, to the best of our knowledge, introduced by Boynton *et al.* (1961), further developed by Shickman (1970), and reported more recently in abstracts by Powers and Robson (1987), Chase *et al.* (1993), Bone and Chen (1995), and Sun *et al.* (1995). In this paradigm, the threshold for a brief flash (the probe) is measured at various phases of a background light that is sinusoidally varied in time. This paradigm was chosen in part because it combines aperiodic (probe) and periodic (background) stimulation and in part because it offers a way to test a model's ability to describe the temporal properties of the adaptation process *per se*. In the first part of this paper, we report data from experiments using this paradigm. In the second part, we show that these data pose difficulties for existing models including the model of von Wiegand *et al.* (1995).

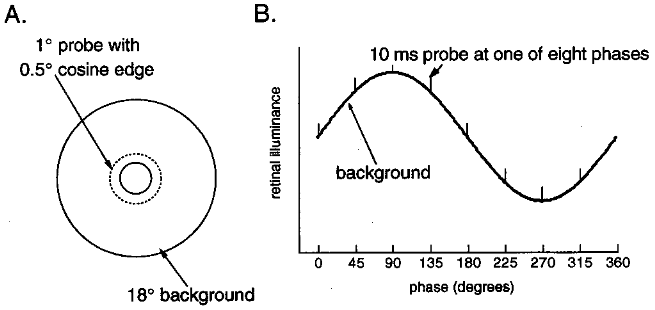

FIGURE 1. The probed-sinewave paradigm. (A) Spatial parameters. (B) Temporal parameters.

EMPIRICAL STUDIES

Methods

Subjects. Four subjects, three females and one male took part in this study, three of them (KF, MC, VMC) in Experiment 1 and two (JG, MC) in Experiment 2. [VMC was a subject in von Wiegand *et al.* (1995) and the parameters of the model in that study were derived from her data.] All four subjects were between 20 and 23 yr of age and had no known color vision defects. Their corrected Snellen acuities were 20/20. All were well-practiced psychophysical observers.

Optical system. High-output, light-emitting diodes (LED) were imaged in the plane of the pupil as 1.5 mm dia circles to provide a Maxwellian view. The radiance of the LEDs was varied over approximately 3 log units using computer controlled, pulse density modulation (Swanson *et al.*, 1987). Fixed neutral density filters were used to extend this range. See von Wiegand (1993) and von Wiegand *et al.* (1995) for more details.

The dominant wavelengths of the nominally red and green LEDs were calculated from the spectra of the LEDs as measured at the observer's eye. The dominant wavelengths were 627 nm (red) and 565 nm (yellow–green) and were essentially on the spectrum locus. The CIE chromaticity coordinates were x: 0.702, y: 0.297 (red LED) and x: 0.412, y: 0.585 (green LED). These values are in general agreement with measured values for LEDs in the literature (Watanabe *et al.*, 1992; Swanson *et al.*, 1987).

Stimuli (the probed-sinewave paradigm). The test flash (probe) was a 1 deg target that had a cosine-amplitude-profile "edge" extending to 2 deg dia. This target was produced by a slide placed in the test channels of the optical system. The slide was a photograph of a printed random-dot pattern with the appropriate density function (von Wiegand *et al.*, 1995). The probe was centered in a circular field (the background) subtending approximately 18 deg [see Fig. 1(A)]. A central fixation line extended vertically from the top of the field to the center of the target. The 18 deg background field was sinusoidally varied, and thresholds were measured with the brief, 10 msec probe flash. The probe was presented at each of eight phases (0, 45, 90, 135, 180, 225, 270, and 315 deg) relative to the sinusoidal modulation of the background

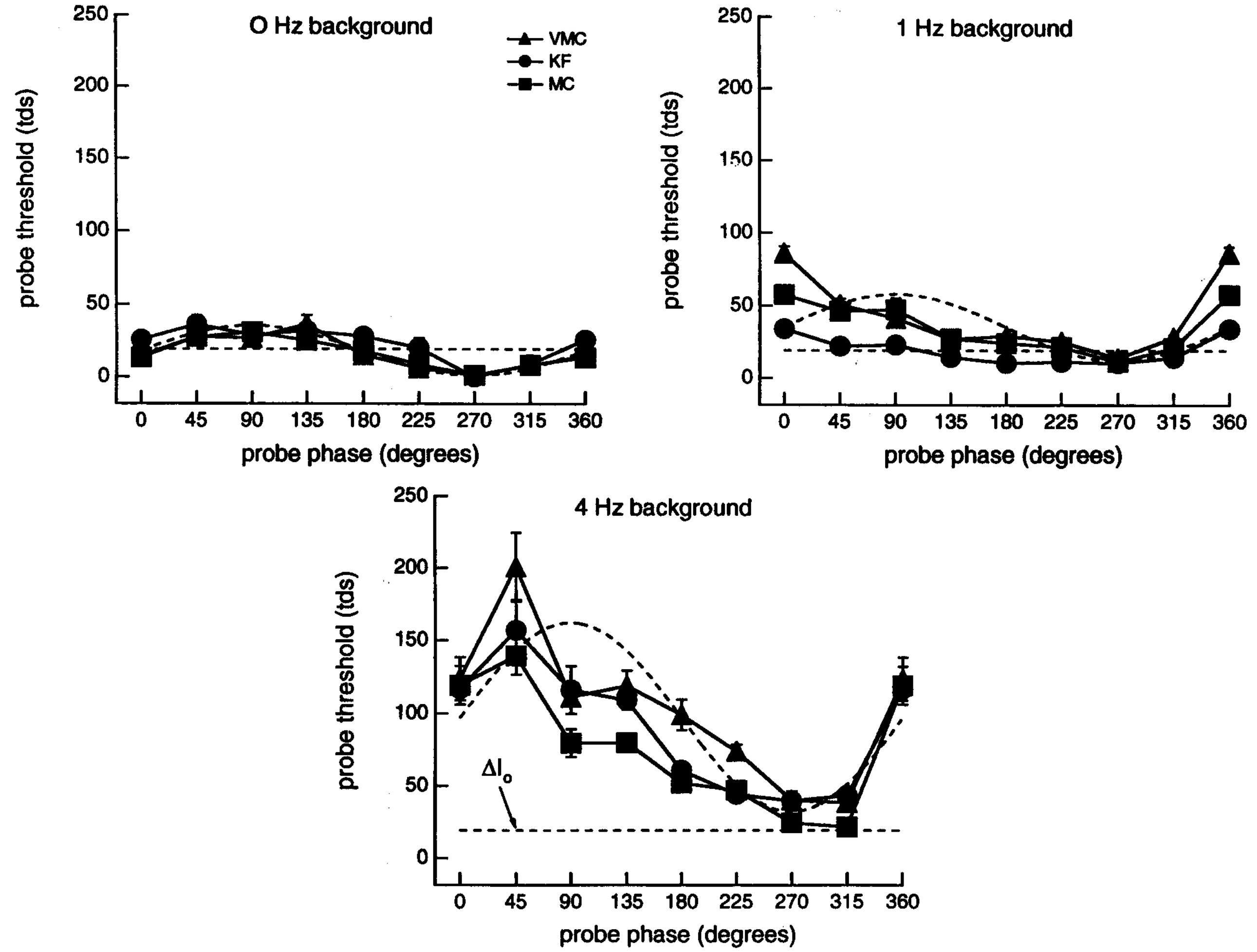

FIGURE 2. Each panel shows the probe threshold (td) for three observers (different symbols) as a function of the phase of background modulation at which the probe was presented. The mean retinal illuminance of the background was 100 td and was modulated at one of three temporal frequencies at 97% contrast. The three panels show the results for the different frequencies of modulation (upper left: 0 Hz; upper right: 1 Hz; lower: 4 Hz). The error bars indicate 1 S.E. The dashed horizontal line in each panel is the probe threshold, ΔI_O, on a steady field of 100 td, averaged across the values for the three observers (KF, 26.6 td; MC, 15.6 td; VMC, 14.7 td). The dashed sinusoidal curves are described in the text.

[see Fig. 1(B)]. The background condition called “0 Hz” is really a set of eight steady backgrounds. Each so-called “phase” in this condition corresponded to the steady field at the luminance that occurs at that phase of a flickering sinewave. (The set of eight steady levels in this condition can be thought of as a very slow sinewave with a frequency approaching 0 Hz.)

With the exception of one set of conditions in Experiment 1 in which the probe and background were green lights, the probe and flash lights were red in both Experiments 1 and 2. The mean illuminance, contrast, and temporal frequencies of the background are detailed in the Results section for both experiments.

Procedure. The psychophysical procedure for the probed-sinewave paradigm was the same in both experiments. Probe thresholds for all eight phases with one background frequency were determined in a session. Within a session, the threshold was determined for one phase at a time. The thresholds for each background frequency were determined in five sessions with the order of the phases different in each session. Sessions for different frequencies were randomly intermixed. At the start of each session, the subject adapted for at least 2 min to a steady field equal to the mean illuminance. This period was followed by 2 min of adaptation to the modulated background to be used in the session. [In the so-called “0 Hz” condition of Experiment 1, the eight phases corresponded to eight steady fields to which the subject adapted for 2 min before the threshold was determined.]

Thresholds were determined using the QUEST psychometric procedure (Watson & Pelli, 1983) and a yes/no paradigm. On each trial, a tone signaled that the stimulus had just been presented and the subject signaled his or her response with a button press. This button press triggered the next stimulus, which then occurred after 500 msec plus a brief delay. The delay was equal to the time needed to finish a cycle and to reach the appropriate phase of the next cycle. Before each QUEST determination of threshold began, the algorithm was provided with an initial estimate of the threshold obtained using the method of adjustment. The QUEST procedure was set up to terminate when the 97.5% confidence interval had decreased to 0.15 log unit.

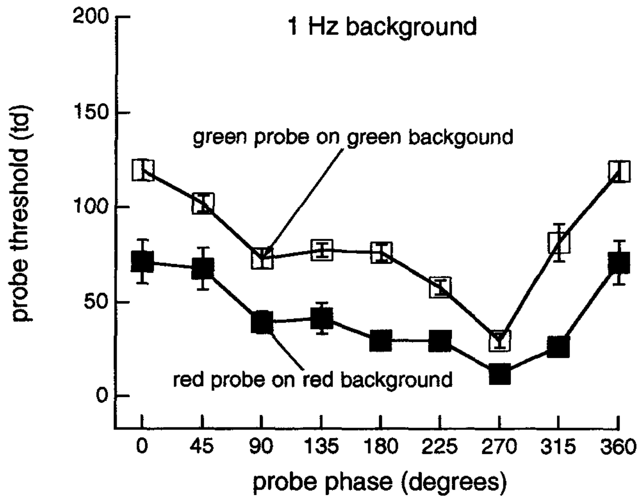

FIGURE 3. The thresholds for a green probe presented upon a green background modulated at 1 Hz and 97% contrast are compared to the results for the equivalent, red probe/red background condition from Fig. 2 (upper right). The error bars indicate 1 S.E.

As part of Experiment 2, a temporal contrast-sensitivity function was determined for the probe. For this experiment only, the homogeneous background was replaced with an annulus. The annulus and probe targets were produced photographically such that the center of the annulus matched the probe's spatial distribution. Thus, when the annulus and probe were of the same illuminance, the entire field appeared homogeneous. This allowed us to obtain a temporal contrast-sensitivity function for the probe surrounded by a field set at the mean illuminace level. Within a session, contrast thresholds were determined for all the temporal frequencies used in the probed-sinewave paradigm of Experiment 2. Five sessions were run, each with a different order of frequencies.

Empirical results

Experiment 1. In Experiment 1, thresholds were determined for the 10 msec, red probe presented at one of eight phases of the sinusoidally modulated, red background. The mean retinal illuminance of the background was 100 trolands, and the contrast was set at 97%. There were three conditions: two were backgrounds modulated at 1 and 4 Hz, and the third was a set of steady backgrounds (called 0 Hz—see Methods section). Figure 2 shows the thresholds for the probe as a function of the phase at which it was presented. Each panel displays the threshold-vs-phase curves for all three subjects (different symbols) for a single background frequency. The horizontal line (ΔI_O) in all the panels is the threshold (averaged across the three observers) for a probe on a steady background at an illuminance equal to the mean of the modulated background. Notice that all the points in the threshold-vs-phase curves for 4 Hz backgrounds are higher then the value of ΔI_O.

The dashed curve in each panel is a sinewave with peak, trough, and dc level set at the average for the three subjects and the phase set to match the stimulus phase. The dc level was determined by taking the mean of the peak and trough thresholds. For the 0 Hz (steady field) condition, the thresholds are approximately described by the sinewave. This is not surprising since the 0 Hz condition consists of a series of steady backgrounds, and 100 td is high enough to be in an approximate Weber range. Hence, the thresholds should be approximately proportional to the steady background and the peaks and troughs in the threshold data should correspond to the maximum (90 deg) and minimum (270 deg) background intensities. However, the data for the 1 and 4 Hz conditions are not well fitted by a sinewave in phase with the stimulus or, indeed, by any sinewave. There is a peak in the data that leads the stimulus peak and is >180 deg out of phase with the trough in the data.

To test whether our results would generalize to lights with different spectral components, the 1 Hz condition was repeated with a green probe on a green modulated background. Figure 3 shows these data for one observer along with her data from Fig. 2. The probed-sinewave data have essentially the same shape when the stimuli are green.

Experiment 2. In Experiment 2, a higher mean luminance (250 td) and a lower modulation contrast (57%) were used along with a wider range of modulation frequencies. Thresholds were obtained for two subjects with a red probe and red background modulations of 1, 2, 4, 8 and 16 Hz. Thresholds, ΔI_O, were also obtained on a steady background at the mean illuminance of 250 td. To better understand the changes with background frequency, one subject was subsequently run with background modulations of 6, 10, and 12 Hz. Figure 4 shows the probe threshold for the two subjects (different symbols) and for different background frequencies (different panels) as a function of the probe phase. The dashed curve again shows a sinewave in phase with the stimulus and adjusted to have a peak, trough, and dc level set at the average of the subjects' data as described in Experiment 1.

There are three salient features of these data. First, as in Experiment 1, the variation in threshold with probe phase is not well described by a sinewave. For the modulation frequencies below 4 Hz, for example, there is >180 deg between the peak and trough in the threshold-vs-phase curve.

Second, at 4–6 Hz there is a dramatic shift in the phase at which the peak probe threshold elevation occurs. While the peak is near 0 or 45 deg for the lower background frequencies, it is around 180 or 225 deg for higher frequencies.

Third, there is what we will call a "dc effect". The dashed horizontal line in each panel of Fig. 4 is the probe threshold, ΔI_O, obtained upon a steady field at the mean illuminance. For a 0 Hz background (see upper left panel of Fig. 2 of Experiment 1), the average or dc level of the threshold-vs-phase curve is at the value of ΔI_O (horizontal dashed line). However, for the other background frequencies used here (1–16 Hz), the average dc level is above the value of ΔI_O, as shown in both Figs 2 and 4.

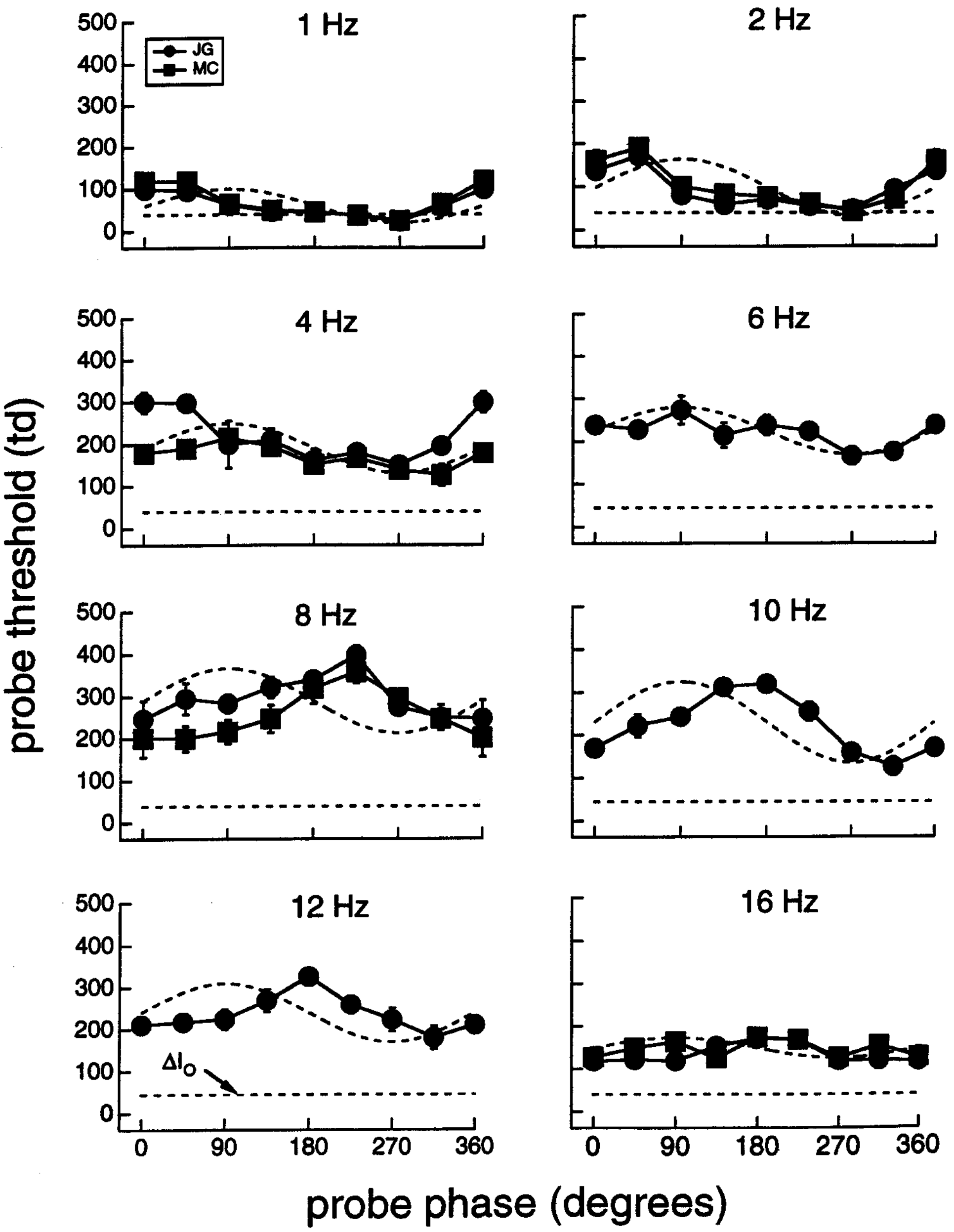

FIGURE 4. Each panel shows the probe threshold (td) for one or both of two observers (different symbols) as a function of the phase of the background modulation at which the probe was presented. The mean retinal illuminance of the background was 250 td and was modulated at one of eight temporal frequencies (different panels) at 57% contrast. The error bars indicate 1 S.E. The dashed horizontal line in each panel is the probe threshold, ΔI_O, on a steady field of 250 td. (ΔI_O equals 44.6 td for JG and 34.4 td for MC.) The dashed sinusoidal curves are described in the text.

This is true even at the highest frequency (16 Hz), where the peak-to-trough variation in probe threshold is quite modest. In fact, for background frequencies from 4 to 16 Hz, the minimum in the threshold-vs-phase curves is not only higher than ΔI_O, the threshold on a steady field at the mean illuminance, but is actually higher than the threshold on a steady field at the peak illuminance. This latter threshold is not shown in the figure but is about 57% above the horizontal dashed line and thus well below the minima of the data.*

To summarize the dc effect, there is an unmodulated (dc) component to the threshold elevation produced by the fluctuating background. The level of this dc component depends on background frequency, being modest for low temporal frequencies, peaking at middle frequencies (8–12 Hz), and diminishing at 16 Hz. This dc elevation is larger than the modulated component for all frequencies >2 Hz.

To dramatize the changes in probe threshold with frequency, the data from Fig. 4 for the 1, 2, 4, 8, and 16 Hz background frequencies are re-plotted in the left

---

*The threshold on a steady field at the peak illuminance was not measured. But we can infer that it would be about 57% higher than the threshold on a steady field at the mean illuminance because the peak illuminance was 57% higher than the mean illuminance of the background in Experiment 2 and the illuminances involved (around 250 td) should be in the Weber region.

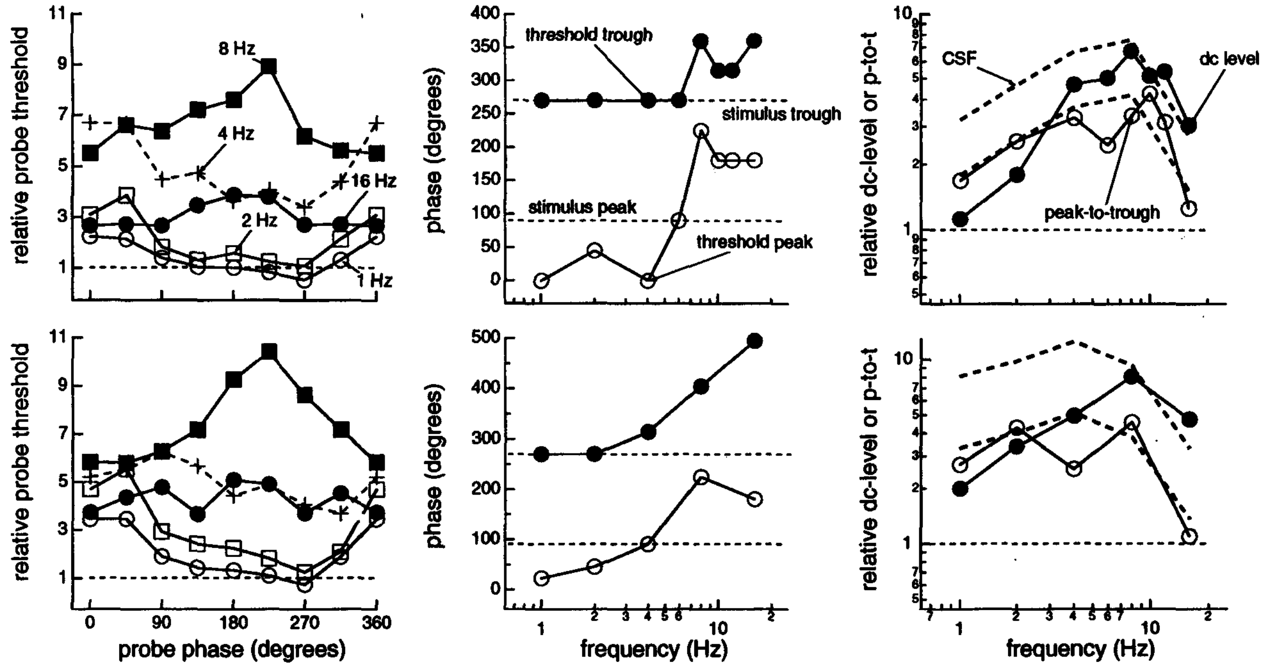

FIGURE 5. Left panels, the probe thresholds from Fig. 4 for five background modulation frequencies are shown expressed relative to the probe threshold, ΔI_O, on a steady field of 250 td. (That is, the probe threshold on the modulated background was divided by the probe threshold on a steady background of 250 td.) Middle panels: the phase at which the peak (open symbols) or trough (filled symbols) occurs in the data is shown as a function of the frequency of the background modulation. Right panels: the relative peak-to-trough threshold difference and relative dc level are shown as a function of the frequency of background modulation. [That is, the peak-to-trough threshold difference in td and dc level (mean of peak and trough thresholds in td) were divided by ΔI_O, the probe threshold on a steady background of 250 td.] The dashed curve is the subject's temporal contrast sensitivity function (TCSF) positioned to coincide with the high frequency limb of the data. The upper panels contain the data for subject JG (circles in Fig. 4) and the lower panels the data for subject MC (squares in Fig. 4).

panels of Fig. 5 for each subject (JG top; MC bottom). In these graphs the thresholds are expressed relative to ΔI_O, the probe threshold on a steady field of the same mean illuminance. For example, a relative probe threshold of two indicates that the probe threshold was elevated by a factor of two over its value against a steady field at the same mean luminance. It is clear in this figure that the dc level in the threshold-vs-phase curves first increases as the frequency of the background increases and then decreases for the highest frequency (16 Hz). It is easy to see also that the phase of the peak changes with frequency.

The middle panels in Fig. 5 show the position of the peak and the trough in the data. The peaks and troughs are clearly not 180 deg apart, the deviations from 180 deg being especially large for the frequencies below 6 Hz. In addition, the data show a striking shift in the position of the peaks and troughs at around 4–8 Hz.

In the right-hand panels of Fig. 5, the open symbols are the differences between the peak and trough thresholds from the threshold-vs-phase curves of Fig. 4 expressed relative to ΔI_O, as in the left-hand panels. These relative peak–trough differences provide a measure of the degree to which the background modulates the probe threshold. The filled symbols in these panels are the dc (or unmodulated) levels (calculated as in Experiment 1 as the mean of the peak and trough thresholds) for the same threshold-vs-phase curves of Fig. 4 and are expressed relative to ΔI_O. The dashed curves labeled CSF are the subject's temporal contrast sensitivity function for the probe. The contrast-sensitivity function has been shifted to coincide with the open or closed symbols above 8 Hz. To a first approximation, the peak-to-trough difference in the probed-sinewave data follows the temporal contrast-sensitivity function. The dc level in the probed-sinewave data, however, shows a more extreme low-frequency decline. In other words, the threshold-vs-phase curves are dominated by a modulated component (a large peak-trough difference) at lower temporal frequencies of background but by an unmodulated component (a threshold elevation maintained throughout the cycle of the sinusoidal background) at higher temporal frequencies.

Discussion of empirical studies

The probed-sinewave paradigm provides a measure of the temporal dynamics of the light adaptation process. If the adaptation changes were instantaneous, then the probed-sinewave data for all background modulations would be similar to the 0 Hz (steady) condition; the peaks and troughs in the data would correspond to those in the stimulus and the dc level would not change with the frequency of the background. The experimental results, however, indicate that some aspects of the adaptation processes are relatively slow. The dc level is higher than the threshold for the mean illuminance level even for the

1 Hz modulation (see dashed lines in Figs 2 and 4). The results also suggest that some changes with adaptation are relatively fast. Background frequencies as high as 8–12 Hz dramatically modulate probe threshold and even the highest frequency used, 16 Hz, produces some modulation of probe threshold.

Others have suggested that the processes involved in light adaptation can involve both relatively fast and relatively slow mechanisms [see for example, Baker (1949); Hayhoe *et al.* (1987, 1992); Geisler (1981, 1983); Adelson (1982); and General Discussion]. This work, however, involved experimental paradigms with aperiodic test and adapting lights. Relatively few studies have used a probed-sinewave paradigm similar to the one used here. The first study to our knowledge was that of Boynton *et al.* (1961). The conditions of their study differed from ours in a number of ways. Most important, they used shorter-duration probes (<3 msec), 100% square wave modulation, and only two background frequencies, 15 and 30 Hz. As in the present study, Boynton *et al.* found a large shift in the dc level relative to the steady field, but, they also found a substantial, modulated component in the threshold-vs-phase curve and these probe thresholds approximately followed the modulation of the background at both 15 and 30 Hz with very little phase shift. That their modulated component at 15 Hz was larger than ours at 16 Hz is probably due to their higher-contrast background and shorter-duration probe. Although our results suggest a peak threshold elevation at a probe phase near 180 deg and theirs near 45 or 90 deg, their conditions are sufficiently different from ours and the modulation of our thresholds at 16 Hz sufficiently small and variable that it is hard to determine with any certainty whether our results are in disagreement with their findings.

In contrast to the Boynton *et al.* (1961) study which used very high temporal frequencies and square-wave backgrounds, Shickman (1970) used six low temporal frequencies (between 3.1 and 10 Hz) and sinusoidally modulating backgrounds. In many ways, Shickman's results agree with ours at the same frequencies. In particular, at these low temporal frequencies, the plots of threshold-vs-phase are decidedly nonsinusoidal; there is a dc component as well as a modulated component; the peak in the threshold-vs-phase curve leads the stimulus peak; and finally, as temporal frequency gets higher, the peak in Shickman's curves begins to move to higher phases as does ours. Our results at these low temporal frequencies differ in at least two ways from Shickman's. First, Shickman's data at 10 Hz is more like our data at lower temporal frequencies. Most of Shickman's data were collected at 1280 td and 100% contrast whereas most of our data were collected at 250 td and 57% contrast. Shickman showed some data at lower luminance and at lower contrasts, although not both at once. But, for either lower luminance or lower contrast, the data at 10 Hz began to look somewhat more like ours. Second, especially for one of Shickman's observers (DB in Fig. 5), there is a clear indication of two peaks in the threshold-vs-phase curves, one of which, like ours, leads the stimulus peak and the other of which is about 180 deg later. Two peaks were also reported by Maruyama and Takahashi (1977) for the two frequencies, 2 and 10 Hz, that they studied. It is clear in both of these studies that the appearance of two peaks is more or less obvious depending upon conditions and observers. It is not easy to discern two peaks in our data. This difference is probably due to one or more of the differences between the conditions of our studies which include: psychophysical method (adjustment vs forced-choice staircases), spatial paradigm (sharp-edged vs cosine-edged test), duration of probe (1–2 msec vs 10 msec), and spectral composition (tungsten and glow modulator white vs red LED).

Likewise, there are points of apparent agreement and disagreement with two other studies that have used the probed-sinewave paradigm and sinusoidal modulation (Powers & Robson, 1987; Bone & Chen, 1995). As in the present study, Powers and Robson (1987) found a dc component in the threshold-vs-phase curves at medium frequencies (largest at 8 Hz). And Bone and Chen (1995) found that the phase of the peak probe threshold increased as the frequency of the background was increased from 5 Hz, the lowest they used, to 45 Hz and that the variations were not well fitted by a sinewave under some conditions. Unlike the present study, Powers and Robson did not report a phase shift at all and both studies report a sinewave variation in probe thresholds under conditions where we find that the data deviate from a sinewave. It is difficult to pinpoint the key differences since these studies are only available in the form of abstracts.

One point of agreement among all these studies is the elevation of the dc level. As discussed above (see Fig. 5), the dc level in the threshold-vs-phase curves is elevated above the threshold (ΔI_O—dashed horizontal line) on a steady field at the mean background illuminance and above the threshold for a steady field at the peak background illuminance (which would be at most 57% above the dashed line—see previous footnote). To some, this may be reminiscent of the phenomenon of brightness enhancement. Brightness enhancement refers to an effect in which the brightness of an intermittent light appears greater than the brightness of a steady field with an intensity equal to the peak of the flashes (e.g. Bartley, 1938). The frequencies most effective at raising the dc level in the present study roughly correspond to the frequencies that produce the most enhancement. For the retinal illuminances used here, brightness enhancement is at its maximum around 6–8 Hz (Bartley, 1938; Wasserman, 1966; van der Horst & Muis, 1969). However, the quantitative similarities end there. Both the lower and higher frequencies in the present study are more effective at raising the dc level than would be expected based on brightness enhancement. The discrepancy is particularly obvious at higher frequencies. At 16 Hz, for example, the dc level in the probed-sinewave results is raised above the threshold ΔI_O on a steady field of the mean illuminance and also above that on a steady field of the peak

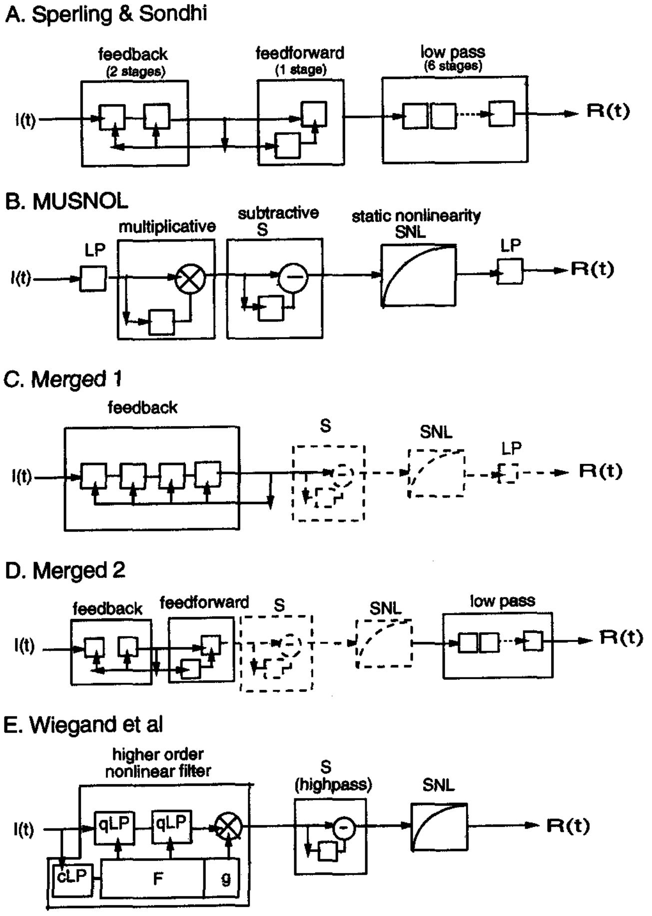

FIGURE 6. Schematics of five computational models that produce a response R as a function of time t given the input intensity I as a function of time. The models are from: (A) Sperling and Sondhi (1968); (B and C) Graham and Hood (1992); and (D) von Wiegand *et al.* (1995). See text for details.

illuminance. Brightness enhancement studies suggest that the 16 Hz field in our study should have a brightness somewhere between these two steady fields (Bartley, 1938; Wasserman, 1966; van der Horst & Muis, 1969). Our stimulus conditions do differ from these studies, but the most notable difference is the blurred edge of our stimuli and Bowen and Pokorny (1978) showed that edge sharpness did not matter in the related brightness enhancement of the Broca–Sulzer phenomenon. Also, Powers and Robson (1987) measured brightness enhancement under the same stimulus conditions as in their probed-sinewave experiment and concluded that the dc elevation in their probed-sinewave results was not well correlated with brightness enhancement across temporal frequency. Thus, we think it likely that the dc effect and brightness enhancement depend, at least in part, on different mechanisms.

The dc effect in the probed-sinewave results may be related to another perceptual nonlinearity: the spatial-frequency doubling in the perceived appearance of sinusoidal gratings (Kelly, 1966, 1981; Pelli, 1986). For spatial frequencies as low as those in our probed-sinewave experiments, there is a transition from a veridical perception to a perception of a doubled spatial frequency at a temporal frequency of 7 or 8 Hz (Kelly, 1966). This transition frequency is similar to that at which phase and dc behavior change in the probed-sinewave results. The spatial-frequency doubling has been tentatively attributed to saturating and/or rectifying processes in the retina (Kelly, 1966, 1981; Pelli, 1986). More information about both the probed-sinewave results and perceived spatial-frequency doubling is needed to determine whether or not they are mediated by the same mechanisms.

THEORETICAL STUDIES

We computed predictions for the probed-sinewave experiments from a number of models of light-adaptation dynamics. Two of these were computational models from the periodic (the Sperling and Sondhi model) and aperiodic (the MUSNOL model) traditions. The other three were merged models containing components from both traditions and were explicitly designed to predict both the dependence of temporal contrast sensitivity on adaptation level (including the high-frequency effect) and the time course of adaptation (including the background-onset effect). These merged models include a frequency-dependent gain-changing component from the periodic tradition (critical in predicting the high-frequency linearity) and a subtractive process followed by a static nonlinearity (SNL) from the aperiodic tradition (critical in predicting the background onset effect). These five models are described in Graham and Hood (1992) and von Wiegand *et al.* (1995). We also computed predictions from a number of other models that are variations on the five mentioned above.

MODELING METHODS

The models

Sperling and Sondhi. The computational model from the periodic tradition that we tested is that proposed by Sperling and Sondhi (1968). It is probably the one that has been applied to the widest range of psychophysical data. Figure 6(A) shows in schematic form the model's three modules: a two-stage feedback module; a one-stage feedforward module; and a six-stage lowpass filter.

MUSNOL (for multiplicative, subtractive, nonlinear). Figure 6(B) is a schematic of the MUSNOL model of Graham and Hood (1992) which is a computational form of models from the aperiodic tradition. It consists of: a one-stage lowpass filter (LP), a multiplicative module, a subtractive module (S), a SNL, and a one-stage LP. The multiplicative module is a process that scales both the probe and background signals by a multiplicative constant. The subtractive module (equivalent to a high-pass filter) removes most of the steady-state response to ambient lights. Similar mechanisms have been suggested for removing the effects of steady fields on color perception (e.g. Hurvich & Jameson, 1958; Walraven, 1976; Shevell, 1977).

Merged 1 and merged 2. By combining elements of

Sperling and Sondhi and MUSNOL, Graham and Hood (1992) created two merged models to predict both the background onset effect and high frequency linearity. Merged 1 resembles MUSNOL, with a four-stage feedback module [solid in Fig. 6(C)] replacing the first two modules. The feedback module allows for adaptation-dependent, temporal frequency sensitivity. Merged 2 has subtractive and SNL modules from MUSNOL [dashed in Fig. 6(D)] sandwiched between the first two modules and the final LP of the Sperling and Sondhi model. The subtractive stage combined with the SNL is necessary to produce the background onset effect in the models from the aperiodic tradition (Graham & Hood, 1992).

von Wiegand et al.. This is the third merged model designed to predict the phenomena from both periodic and aperiodic paradigms and the only one to be quantitatively fitted to data. As seen in Fig. 6(E), it has a highpass filter (effectively a subtractive module) and a SNL. The first module, a higher order nonlinear filter, provides a frequency-dependent gain controlling process that is dependent upon background illuminance. This module consists of two second order quadratic LPs (qLP) and a control signal that is lowpass filtered (cLP). This model is fully described in von Wiegand *et al.* (1995). Higher order filters have been used in other models of adaptation (e.g. Kelly, 1971; Tranchina & Peskin, 1988; Purpura *et al.*, 1990).

Variant. We also used a number of variants of the above models in which one or more of the parameter values (including the form of the SNL) had been changed. Some of the more revealing variants will be described below.

Decision rule. For all models we assume a constant-response (peak detection) rule for the threshold decision. In particular, threshold is the value of probe intensity for which ΔR (the response to the background plus probe minus the response to the background) equals a criterion δ.

Predictions

Predicted thresholds for the probed-sinewave paradigm and background modulations of 1, 2, 4, 8, and 16 Hz were generated for each of the five models using MATLAB by Math Works. As in Experiment 2, the mean illuminance was 250 td and the contrast 57%. In addition, the temporal contrast sensitivity function was predicted from each model. The criterion value δ for ΔR was set equal to 0.02, but this value is not critical. Large variations in δ have no effect at all on the predictions as they are plotted below. Further details about the calculations, including the parameter values used, are in Graham and Hood (1992) and von Wiegand *et al.* (1995). Large variations in these parameters do not affect the conclusions below.

THEORETICAL RESULTS

The predictions of the models are shown in Figs 7 and 8, plotted in the same form as in Fig. 5. In the left panels, the predicted probe thresholds are plotted as a function of phase for each of the five background frequencies. The thresholds are expressed relative to ΔI_{O}, the threshold for a probe superimposed on a steady field at the mean illuminance. The horizontal dashed line is the threshold for a probe on a steady background at the mean illuminance (which is 1.0 in this relative form). The middle panels show the phase data as in Fig. 5 (middle panels), and the right panels the amplitude data as in Fig. 5 (right panels), plotted relative to ΔI_{O}.

The top row of Fig. 7 shows the predicted results for the von Wiegand *et al.* model. The predicted probed-sinewave curves (left panel) exhibit two peaks, a "frequency-doubling". Although two studies (Maruyama & Takahashi, 1977; Shickman, 1970) discussed above found two peaks in the probed-sinewave data under some conditions, the second peak was not prominent. In any case, these peaks did not fall at the peaks and troughs of the stimulus as predicted by the von Wiegand *et al.* model. Although the double peaks are one of the most salient features of the von Wiegand *et al.* model's predictions, a relatively minor modification of the model can remove the second set of peaks. The frequency doubling occurs because the SNL in the von Wiegand *et al.* model was presumed to be odd-symmetric around the background luminance. As it happens, this odd symmetry is not necessary for the predictions of high-frequency linearity and the background-onset effect. The odd-symmetric SNL can be replaced by a SNL having any form below zero with very little effect on the predictions for the flicker sensitivity or probe-flash paradigms. However, changing the negative half of the SNL has a large effect on the predictions for the probed-sinewave paradigm. The middle panels of Fig. 7 show predictions for the probed-sinewave paradigm from a modified version of the von Wiegand *et al.* model in which the SNL is linear below zero. This modification removes the peak that occurs in the second half of the cycle. The position of the first peak remains at 90 deg (middle panel) for all frequencies. The position of the trough is not well defined since there is very little difference in the probe threshold over a range of phases (indicated by the vertical bars in the figure).

Unlike the data in Fig. 5, the predictions of the von Wiegand *et al.* model, both as originally published or with the modified SNL (Fig. 7, top and middle rows), follow the background reasonably well over the positive portion of the sinusoidal modulation. In particular, the peak threshold elevation coincides with the peak luminance of the stimulus at 90 deg. Further, unlike in the data, there is no unmodulated component in the predicted threshold-vs-phase curves. That is, there is no maintained elevation of probe threshold throughout the cycle of the sinusoidal background. The minimum in the predicted curves equals the threshold on a steady field at the mean illuminance. An associated prediction of this model is that the dc level and peak-to-trough functions should have much the same shape (Fig. 7, right panels) whereas in the data they differ dramatically (Fig. 5, right panel).

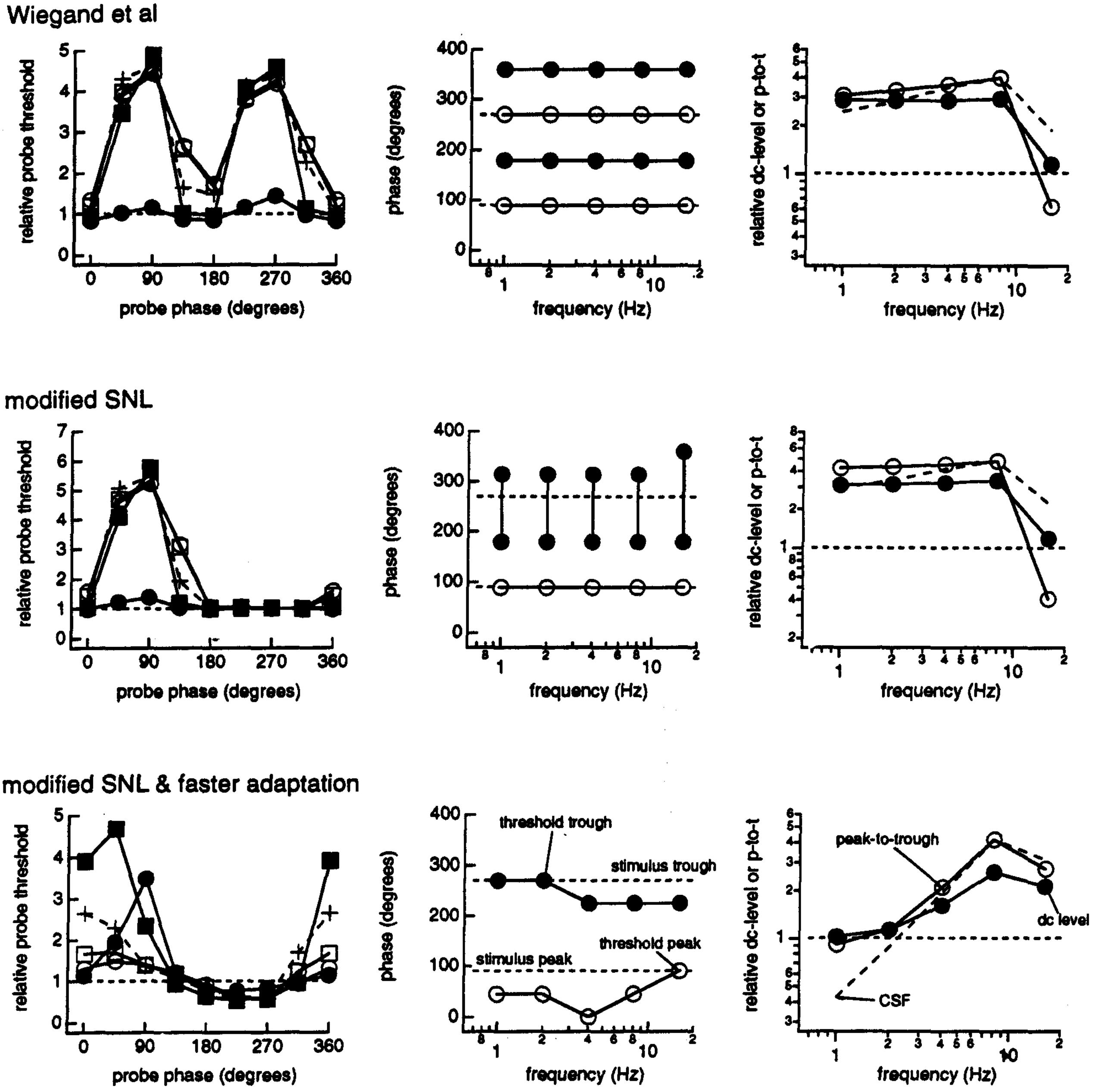

FIGURE 7. First row: Predictions of the Wiegand *et al.* model for probed-sinewave results. The simulated results are presented in the same form as the actual data in Fig. 5. See text for details. Second row: Predictions for a version of the Wiegand *et al.* model in which the SNL was made linear below 0. See text for details. Third row: Predictions for a version of the Wiegand *et al.* model modified by changing the time constants of cLPF and the highpass filter. See text for details.

The model in the bottom row of Fig. 7 is a further modification of the von Wiegand *et al.* model which will be presented in the discussion of the theoretical studies.

Figure 8 shows the predictions of the other four models in the same form as Fig. 7. The results for the two merged models and MUSNOL are similar enough so that they can be summarized together. Although all three predict a change in the position of the peak and trough with frequency (top three rows, middle panels), these shifts are small relative to those seen in the data. As with the von Wiegand *et al.* model and its variants, these models predict no unmodulated component in the threshold-vs-phase curves. Further, the predicted dc level and peak-to-trough functions (Fig. 8, right panels) are, unlike the data, approximately the same. As in the case of the von Wiegand *et al.* model, the frequency doubling visible in these predictions can be removed with a change in the SNL. Although not shown here, this does not improve the models' ability to predict other aspects of the data.

The bottom panels of Fig. 8 show the results for the Sperling and Sondhi model. The predicted thresholds follow the sinusoidal modulation of the background nearly perfectly, that is, adaptation is extremely fast. Thus the predicted peak and trough in the probed-sinewave data always occur at the peak and trough of the stimulus, and there is no unmodulated component.

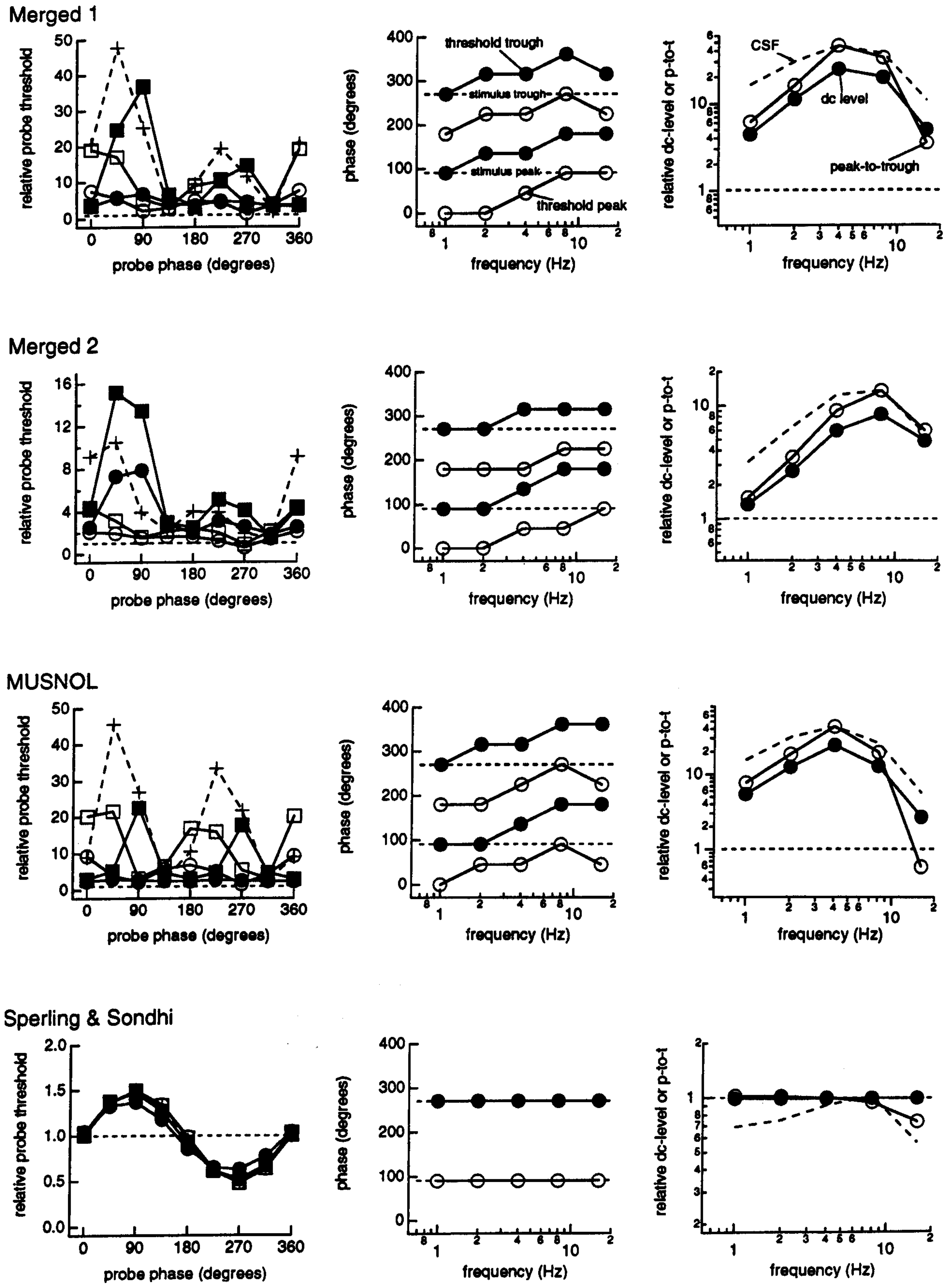

FIGURE 8. Predictions of merged 1 (top row), merged 2 (second row), MUSNOL (third row), and Sperling and Sondhi (bottom row) models presented as in Fig. 7. See Fig. 7 caption and text for details.

Accordingly, the dc level is always at the threshold for a probe on a steady field of the mean illuminance. None of these predictions bear much resemblance to the data.

DISCUSSION OF THEORETICAL STUDIES

The three merged models and the MUSNOL model (but not the Sperling and Sondhi model) correctly predict one key aspect of the data. All predict that the plot of peak–trough amplitude vs frequency curves (open symbols in right panels of Fig. 5) has about the same shape as the temporal contrast sensitivity function (dashed curve labeled CSF). The models that correctly predict this aspect of the data all have an SNL. Presumably, the higher the sensitivity to a given temporal frequency, the greater the amplitude of the signal into the SNL from the modulated background. Because the SNL is compressive, the greater the background's response, the smaller will be the incremental response to the probe and the higher the probe threshold.

Interestingly, the Sperling and Sondhi model predicts a contrast-sensitivity function that is actually narrower (on both the low-frequency and high-frequency ends) than the predicted peak-trough amplitude in the probed-sinewave experiment. In the extreme, therefore, one could find sinusoidal backgrounds that, according to this model, would modulate the probe thresholds although the flicker in the background would be invisible to the observer. In fact, Boynton *et al.* (1961) reported such a condition for high-frequency flicker. The Sperling and Sondhi model makes this prediction on the high-frequency end because the final stages of lowpass filtering attenuate the flicker after the flickering background has had its adapting effect. Other models that have final low-pass filtering could also make such a prediction under the right conditions.

Although all the models except Sperling and Sondhi predict one aspect of the data (i.e. the similarity of the peak-trough flicker sensitivity functions), they all fail to predict two important aspects: the phases and the dc levels of these same curves. We discuss each of these failures briefly.

First, none of the models predicts the abrupt change in the position of the major peak from near 0 to near 180 deg as background frequency is increased. We tried without success to find parameters of the various modules of these models that would produce satisfactory phase shifts. A natural place to start was the time course of the mechanisms controlling adaptation. In previous work, a range of time constants has been used for both multiplicative and subtractive processes (Shevell, 1977; Hayhoe *et al.*, 1987; Walraven & Valeton, 1984; Hayhoe *et al.*, 1992; Olson *et al.*, 1993). In the von Wiegand *et al.* model it is possible to manipulate the "speed of adaptation" *per se* by changing the time constant of the control low-pass filter (cLPF) or that of the high-pass filter (the subtractive process). If adaptation is made faster by either method, then the predictions of von Wiegand *et al.* look more like the predictions of the two merged models, although the details of the changes and their causes are different with each method. In either case, the predictions are no closer to the data than are those of the merged models. The lower panels of Fig. 7 show our most successful attempt. Here the version of the von Wiegand *et al.* model in the middle row of Fig. 7 is further modified by shortening both time constants controlling the speed of adaptation (the time constants of the control signal, cLP, in the first module and that of the highpass filter in the subtraction module). This modified model predicts modest phase shifts that are too small in the case of the peak and in the wrong direction in the case of the trough. Two other changes that we considered in some detail are in the form of the SNL and the detection criterion. Assuming a peak-to-trough detector, rather than a peak detector, changes the predictions but the agreement with the data is improved little, if at all. Likewise, although changes in the SNL remove the frequency doubling, we were unable to find a plausible SNL that substantially improved the predictions in any other respects.

The second aspect of the data that the models fail to capture is the dc effect—the presence of an unmodulated component, especially at medium to high temporal frequencies. In the data, the dc level does not follow the temporal contrast sensitivity function, CSF, while the peak-to-through difference does. In the von Wiegand *et al.*, MUSNOL and the merged models (including the versions with linear-negative SNLs), the dc level essentially follows the peak–trough difference. This occurs because the probe threshold-vs-phase curves resemble a half-wave rectified (for the linear-negative SNL) or full-wave rectified (original SNL) periodic wave; thus, the dc level will be proportional to the peak–trough amplitude. It seems unlikely that any change short of adding another component will allow any of these models to predict the dc levels.

GENERAL DISCUSSION

Our purpose here was to explore a relatively unused paradigm, the probed-sinewave paradigm, as a vehicle for distinguishing among candidate models of light adaptation. The paradigm produced orderly data with clear features. The candidate light-adaptation models, however, were unable to predict these features and our attempts to rescue them by changing parameter values and the decision rule were unsuccessful. While it is plausible that other modifications would produce predictions closer to the data, it is hard to believe these models can be rescued without adding additional components. For discussion, we divide these possible components into those that seem to require an additional channel vs those components that can be added to the single-channel of the models in Fig. 6.

Possible additional channels

The models considered here represent the visual system as a single channel sensitive to the full visible range of spatial frequency, temporal frequency, and spectral wavelength. However, considerable evidence exists for multiple, wavelength-selective channels (i.e. the three cone types and three opponent-color mechanisms in the photopic range) and also for multiple, spatial-frequency channels [for a review see Graham (1989)]. Interestingly, Kortum and Geisler (1995) have recently shown that MUSNOL can be extended to multiple, spatial-frequency channels with the same multiplicative and subtractive stages; only the SNL needs to be modified. Although the evidence suggests much less selectivity for temporal frequency than for spatial frequency, it also suggests that more than one temporal frequency channel exists. Many have proposed the existence of two temporal-frequency, psychophysical channels, particularly at low spatial frequencies like those used here. The channels were originally referred to in the 1970s as "sustained" vs "transient" channels and are now thought to result from the differential properties of neurons in M and P pathways in the primate [see review in Graham (1989) section 12.3.1; Kaplan *et al.* (1990); Merigan & Maunsell (1993)]. There may be as many as three temporal-frequency channels at low spatial frequencies [see review in Graham (1989); Mandler & Makous (1984); Hess & Snowden (1992)]. Further, a number of people have proposed channels sensitive to different temporal phases, i.e. "on" vs "off" channels [see the next paragraph and the review in Schiller (1992)]. The probe to be detected in our experiments had a constant spatial, temporal, and wavelength composition. On the one hand, therefore, a single channel may always be responsible for its detection. On the other hand, the presence of the sinusoidally varying, adapting background may change the relative sensitivities of different channels, allowing one channel to be more sensitive for low-temporal-frequency backgrounds and another channel for high temporal-frequency backgrounds. Such a shift might underlie the change in the dc level and phase with background frequency. At this point in our investigations, however, we know of no compelling argument for or against any particular shift among channels, and we know of no evidence that a particular shift would produce the dc effect and phase shifts seen here.

Possible additional components

Rather than a shift among channels, additional components (processes) within a single channel may lead to the dc effect and phase shifts in the probed-sinewave paradigm. Several possibilities come to mind. One is to introduce a second multiplicative or subtractive process since there is evidence for more than one multiplicative and subtractive process with separate temporal properties (Hayhoe *et al.*, 1987, 1992; Hayhoe, 1990; Kortum & Geisler, 1995). A second is to introduce a process that will produce an asymmetry between the on- and off-responses of the single channel. There is evidence that both on- and off-responses are contributing to the shape of the probed-sinewave data. By comparing thresholds on backgrounds modulated with square wave and sinusoidal variations, Maruyama and Takahashi (1977) associated the two peaks in their probed-sinewave data with the on- and off-threshold elevations observed in the Crawford paradigm. These on- and off-effects may be due to two channels as discussed above or may be a manifestation of the changes in a single channel. The properties of physiological on- and off-responses are known to be different (e.g. Spitzer *et al.*, 1993; Zemon *et al.*, 1988) and Shickman (1970) suggested that these properties might account for some features of his results. Further, a variety of psychophysical studies using the probe-flash paradigm have argued that the time course of the adaptation mechanisms are different at the onset as opposed to the offset of an adapting background (e.g. Adelson, 1982; Geisler, 1981, 1983; Hayhoe *et al.*, 1987, 1992). For example, Hayhoe *et al.* (1987) found that the multiplicative process in models like MUSNOL [Fig. 6(B)] was complete within 25–50 msec after light onset but took well over 200 msec to decay at light offset. Perhaps the fact that our data do not follow a sinewave reflects the differential time courses at onset vs offset. Likewise, the elevated dc level may reflect the combined effect of on- and off-responses with different temporal characteristics. To introduce asymmetry between onset and offset in the von Wiegand *et al.* model, for example, the adaptation pathway might be expanded to include some storage and rectification of the control signal (von Wiegand *et al.*, 1995). Alternatively, the straight-through pathway in any of the models might be modified to include some storage as proposed in the model of Spitzer *et al.* (1993).

A third possibility is to introduce a process which readjusts the channel's gain based on an average of the recent stimulus contrast. This process has been called a "contrast-gain control" and is to be distinguished from a process that readjusts the gain based on average recent luminance (as conventional light-adaptation processes are assumed to do). Contrast-gain control has been studied in the retina (e.g. Benardette *et al.*, 1992; Shapley & Victor, 1981) and in the cortex (e.g. Albrecht & Geisler, 1991; Albrecht & Hamilton, 1982; Carandini *et al.*, in press; Ohzawa *et al.*, 1985; see Bonds, 1993 for a review). We suspect that the background-onset-effect and the probed-sinewave results are primarily retinal due to the spatial configuration in our experiments. In particular, for adapting fields much larger than the test field as in our experiments, Battersby and Wagman (1962) showed that there is very little interocular transfer of the background-onset effect. Therefore, the retinal contrast-gain control seems a more promising candidate than the cortical one for our probed-sinewave results. In primates, the retinal contrast-gain mechanism is known to operate in M cells, but not in P cells (Benardette *et al.*, 1992). The test probe in our experiments is likely to be detected by M cells since it contains low spatial frequencies and high temporal frequencies (e.g. Kaplan & Shapley, 1986; Lee *et al.*, 1990; Merigan & Maunsell, 1993; Schiller *et al.*, 1990). However, whether the contrast gain in primate

M cells has the properties necessary to explain our probed-sinewave results is not known at this time.

While this discussion suggests a number of plausible directions for future work, it is not at all clear which direction or model will ultimately prove most successful. We started with a paradigm we thought would be a strong test of existing models; the test turned out to be even stronger than we expected.

REFERENCES

Adelson, E. H. (1982). Saturation and adaptation in the rod system. *Vision Research, 22*, 1299–1312.

Albrecht, D. G. & Geisler, W. S. (1991). Motion selectivity and the contrast-response function of simple cells in the visual cortex. *Visual Neuroscience, 7*, 531–546.

Albrecht, D. G. & Hamilton, D. B. (1982). Striate cortex of monkey and cat: Contrast response function. *Journal of Neurophysiology, 48*, 217–237.

Baker, H. D. (1949). The course of foveal light adaptation measured by the threshold intensity increment. *Journal of the Optical Society of America, 39*, 172–179.

Bartley, S. H. (1938). Subjective brightness in relation to flash rate and the light–dark ratio. *Journal of Experimental Psychology, 23*, 313–319.

Battersby, W. S. & Wagman, I. H. (1962). Neural limitations of visual excitability. IV: Spatial determinants of retrochiasmal interaction. *American Journal of Physiology, 203*, 359–365.

Baylor, D. A., Hodgekin, A. L. & Lamb, T. D. (1974). Reconstruction of the electrical responses of turtle cones to flashes and steps of light. *Journal of Physiology, 242*, 759–791.

Benardette, E. A., Kaplan, E. & Knight, B. W. (1992). Contrast gain control in the primate retina: P cells are not X-like, some M cells are. *Visual Neuroscience, 8*, 483–486.

Bonds, A. B.(1993) The encoding of cortical contrast gain control. In Shapley, R. & Lam, D. M. (Eds), *Contrast sensitivity: Proceedings of the Retina Research Foundation symposia*. Cambridge, MA: MIT Press.

Bone, R. A. & Chen, Y. P. (1995). Improved temporal gain and phase measurements (5–45 Hz) leading to a triphasic impulse response. *Investigative Ophthalmology and Visual Science, 36* suppl.-abstract, S906.

Bowen, R. W. & Pokorny, J. (1978). Target edge sharpness and temporal brightness enhancement. *Vision Research, 18*, 1691–1695.

Boynton, R. M. & Kandel, G. (1957). On responses in the human visual system as a function of adaptation level. *Journal of the Optical Society of America, 47*, 275–286.

Boynton, R. M., Sturr, J. F. & Ikeda, M. (1961). Study of flicker by increment threshold technique. *Journal of the Optical Society of America, 51*, 196–201.

Carandini, M., Heeger, D. J. & Movshon, J. A. (in press). Linearity and gain control in V1 simple cells. In Jones, E. G. & Ulinski, P. S. (Eds), *Cerebral cortex*, Vol. X, Cortical models. New York: Plenum Press.

Chase, V. M., von Wiegand, T. E., Hood, D. C. & Graham, N. (1993). Exploring the dynamics of light adaptation using a sinusoidally modulated background and a probe. *Investigative Ophthalmology and Visual Science, 34*, 1036.

Crawford, B. H. (1947). Visual adaptation in relation to brief conditioning stimuli. *Proceedings of the Royal Society, B, 134*, 283–302.

De Lange, H. (1952). Experiments on flicker and some calculations on an electrical analogue of the foveal systems. *Physica, 18*, 935–950.

De Lange, H. (1958). Research into the dynamic nature of the human fovea–cortex systems with intermittent and modulated light. *Journal of the Optical Society of America, 48*, 779–789.

Dodge, F. A., Knight, B. W. & Toyoda, J. (1968). Voltage noise in *Limulus* visual cells. *Science, 160*, 88–90.

Finkelstein, M. A., Harrison, M. & Hood, D. C. (1990). Sites of sensitivity control within a long-wavelength cone pathway. *Vision Research, 30*, 1145–1158.

Fuortes, M. G. F. & Hodgekin, A. L. (1964). Changes in time scale sensitivity in the ommatidia of Limulus. *Journal of Physiology, 172*, 239–263.

Geisler, W. S. (1978). Adaptation, afterimage and cone saturation. *Vision Research, 18*, 279–289.

Geisler, W. S. (1979). Initial image and afterimage discrimination in the human rod and cone systems. *Journal of Physiology, 294*, 165–179.

Geisler, W. S. (1981). Effects of bleaching and backgrounds in the flash response of the cone system. *Journal of Physiology, 312*, 413–434.

Geisler, W. S. (1983). Mechanisms of visual sensitivity: Backgrounds and early dark adaptation. *Vision Research, 23*, 1423–1432.

Graham, N. (1989). *Visual pattern analyzers*. New York: Oxford University Press.

Graham, N. & Hood, D. C. (1992). Modeling the dynamics of light adaptation: The merging of two traditions. *Vision Research, 32*, 1373–1393.

Hayhoe, M., Benimoff, N. I. & Hood, D. C. (1987). The time-course of multiplicative and subtractive adaptation processes. *Vision Research, 27*, 1981–1996.

Hayhoe, M. M. (1990). Spatial interactions and models of adaptation. *Vision Research, 30*, 957–965.

Hayhoe, M. M., Levin, M. E. & Koshel, R. J. (1992). Subtractive processes in light adaptation. *Vision Research, 32*, 323–333.

Hess, R. F. & Snowden, R. J. (1992). Temporal properties of human visual filters: Number, shapes and spatial covariation. *Vision Research, 32*, 47–59.

Hood, D. C. (1978). Psychophysical and electrophysiological tests of physiological proposals of light adaptation. In Armington, J., Krauskopf, J. & Wooten, B. (Eds), *Visual psychophysics: Its physiological basis*. New York: Academic Press.

Hood, D. C. & Finkelstein, M. A. (1986). Sensitivity to light. In Boff, K. R., Kaufman, L. & Thomas, J. P. (Eds), *Handbook of perception and human performance, Vol. I: Sensory processes and perception.* New York: John Wiley and Sons.

Hood, D. C., Finkelstein, M. A. & Buckingham, E. (1979). Psychophysical tests of models of the response function. *Vision Research, 19*, 401–406.

Hood, D. C., Ilves, T., Maurer, E., Wandell, B. & Buckingham, E. (1978). Human cone saturation as a function of ambient intensity: A test of models of shifts in the dynamic range. *Vision Research, 18*, 983–993.

van der Horst, G. J. C. & Muis, W. (1969). Hue shift and brightness enhancement of flickering light. *Vision Research, 9*, 953–963.

Hurvich, L. M. & Jameson, D. (1958). Further development of a quantified opponent-color theory. *Vision problems of color II* (pp. 691–723). London: HMSO.

Kaplan, E., Lee, B. B. & Shapley, R. M. (1990). New views of primate retinal function. In Osborne, N. & Chader, G. (Eds), *Progress in retinal research*, Vol. 9. Oxford: Pergamon.

Kaplan, E. & Shapley, R. M. (1986). The primate retina contains two types of ganglion cells with high and low contrast sensitivity. *Proceedings of the National Academy of Sciences USA, 83*, 2755–2757.

Kelly, D. H. (1961). Visual responses to time-dependent stimuli: II. Single channel model of the photopic visual system. *Journal of the Optical Society of America, 51*, 747–754.

Kelly, D. H. (1966). Frequency doubling in visual responses. *Journal of the Optical Society of America, 56*, 1628–1633.

Kelly, D. H. (1971). Theory of flicker and transient responses: I. Uniform flicker. *Journal of the Optical Society of America, 61*, 537–546.

Kelly, D. H. (1981). Nonlinear visual responses to flickering sinusoidal gratings. *Journal of the Optical Society of America, 71*, 1051–1055.

Kelly, D. H. & Wilson, H. R. (1978). Human flicker sensitivity: Two stages of retinal diffusion. *Science, 202*, 896–899.

Kortum, P. T. & Geisler, W. S. (1995). Adaptation mechanisms in spatial vision—II. Flash threshold and background adaptation. *Vision Research, 35*, 1595–1609.

Lee, B. B., Pokorny, J., Smith, V. C., Martin, P. R. & Valberg, A.

(1990). Luminance and chromatic modulation sensitivity of macaque ganglion cells and human observers. *Journal of the Optical Society of America, 7,* 2223–2236.

Mandler, M. B. & Makous, W. (1984). A three channel model of temporal frequency perception. *Vision Research, 24,* 1818–1887.

Maruyama, K. & Takahashi, M. (1977). Wave form of flickering stimulus and visual masking function. *Tohoku Psychologica Folia, 36,* 120–133.

Matin, L. (1968). Critical duration, the differential luminance threshold, critical flicker frequency, and visual adaptation: A theoretical treatment. *Journal of the Optical Society of America, 58,* 404–415.

Mejia-Monasterio, N. A. & Gaudiano, P. (1995). A calcium-dependent mechanism improves light adaptation in a simulated photoreceptor. *Investigative Ophthalmology and Visual Science, 36* suppl-abstract, S664.

Merigan, W. H. & Maunsell, J. H. R. (1993). How parallel are the primate visual pathways?. *Annual Review of Neurosciences, 16,* 369–402.

Ohzawa, I., Sclar, G. & Freeman, R. D. (1985). Contrast gain control in the cat's visual system. *Journal of Neurophysiology, 54,* 651–667.

Olson, J. D., Tulunay-Keesey, Ü. & Saleh, B. E. A. (1993). Fading time of retinally-stabilized images as a function of background luminance and target width. *Vision Research, 33,* 2127–2138.

Pelli, D. G. (1986). Bright areas appear magnified: A visual saturation? *Investigative Ophthalmology and Visual Science, 27* suppl.-abstract, 226.

Powers, M. K. & Robson, J. G. (1987). Sensitivity changes induced by temporal modulation of a background. *Investigative Ophthalmology and Visual Science, 28* suppl.-abstract, 357.

Purpura, K., Tranchina, D., Kaplan, E. & Shapley, R. M. (1990). Light adaptation in the primate retina: Analysis of changes in gain and dynamics of monkey retinal ganglion cells. *Visual Neuroscience, 4,* 75–93.

Roufs, J. A. J. (1972a) Dynamic properties of vision—I. Experimental relationship between flicker and flash thresholds. *Vision Research, 12,* 261–278.

Roufs, J. A. J. (1972b) Dynamic properties of vision—II. Theoretical relationship between flicker and flash thresholds. *Vision Research, 12,* 279–292.

Schiller, P. H. (1992). The on and off channels of the visual system. *TINS, 15,* 86–92.

Schiller, P. H., Logothetis, N. K. & Charles, E. R. (1990). Functions of the colour-opponent and broad-band channels of the visual system. *Nature, 343,* 68–70.

Shapley, R. M. & Enroth-Cugell, C. (1984). Visual adaptation and retinal gain controls. In Osborne, N. N. & Chader, G. J. (Eds), *Progress in retinal research,* Vol. 3 (pp. 263–343). Oxford: Pergamon.

Shapley, R. M. & Victor, J. (1981). How the contrast gain control modifies the frequency responses of cat retinal ganglion cells. *Journal of Physiology, 318,* 161–179.

Shevell, S. K. (1977). Saturation in human cones. *Vision Research, 17,* 427–434.

Shevell, S. K. (1978). The dual role of chromatic backgrounds in color perception. *Vision Research, 18,* 1649–1661.

Shickman, G. M. (1970). Visual masking by low-frequency sinusoidally modulated light. *Journal of the Optical Society of America, 60,* 107–117.

Sperling, G. & Sondhi, M. M. (1968). Model for visual luminance discrimination and flicker detection. *Journal of the Optical Society of America, 58,* 1133–1145.

Spitzer, H., Almon, M. & Sandler, V. M. (1993). A model for detection of spatial and temporal edges by a single X cell. *Vision Research, 33,* 1871–1880.

Sun, V. C. W., Pokorny, J. & Smith, V. C. (1995). Increment thresholds on temporally modulated backgrounds. *Journal of the Optical Society of America,* (meeting) 88.

Swanson, W. H., Ueno, T., Smith, V. C. & Pokorny, J. (1987). Temporal modulation sensitivity and pulse detection thresholds for chromatic and luminance perturbations. *Journal of the Optical Society of America, 4,* 1992–2005.

Tranchina, D., Gordon, J. & Shapley, R. M. (1984). Retinal light adaptation—evidence for a feedback mechanism. *Nature, 310,* 314–316.

Tranchina, D. & Peskin, C. S. (1988). Light adaptation in the turtle retina: Embedding a parametric family of linear models in a single nonlinear model. *Visual Neuroscience, 1,* 339–348.

Wasserman, G. S. (1966). Brightness enhancement in intermittent light: Variation of luminance and light–dark ratio. *Journal of the Optical Society of America, 56,* 242–250.

Walraven, J. (1976). Discounting the background—the missing link in the explanation of chromatic induction. *Vision Research, 16,* 289–295.

Walraven, J. & Valeton, J. M. (1984). Visual adaptation and response saturation. In Van Doorn, A. J., Van de Grind, W. A. & Koenderink, J. J. (Eds), *Limits in perception* (pp. 401–429). Utrecht: VNU Science Press.

Watanabe, T., Mori, N. & Nakamura, F. (1992). A new superbright LED stimulator: Photodiode-feedback design for linearizing and stabilizing emitted light. *Vision Research, 32,* 953–961.

Watson, A. B. (1986). Temporal sensitivity. In Boff, K. R., Kaufman, L. & Thomas, J. P. (Eds), *Handbook of perception and human performance, Vol I: Sensory processes and perception.* New York: John Wiley and Sons.

Watson, A. B. & Pelli, D. G. (1983). QUEST: A Bayesian adaptive psychometric method. *Perception and Psychophysics, 33,* 113–120.

von Wiegand, T. E. (1993). A psychophysically based computational model of the dynamics of light adaptation. Doctoral dissertation. Columbia University. Ann Arbor: University Microfilms International.

von Wiegand, T. E., Hood, D. C. & Graham, N. V. (1995). Testing a computation model of light-adaptation dynamics. *Vision Research, 35,* 3037–3051.

Wilson, H. R. (1995). Physiological predictions of a dynamic model for retinal function. *Investigative Ophthalmology and Visual Science, 36* suppl.-abstract, S16.

Zemon, V., Gordon, J. & Welch, J. (1988). Asymmetries in on and off visual pathways of humans revealed using contrast-evoked cortical potentials. *Visual Neuroscience, 1,* 145–150.

Acknowledgements—This research was supported by National Eye Institute Grants EY-02115 and EY-08459 to D. Hood and N. Graham, respectively. We thank Joel Pokorny and William Swanson for their assistance in constructing the PDM stimulator, Janet Go, Malancha Chanda, and Marsha Goodman for their help in running the experiments, and Maureen Powers, John Robson, and Robert Shapley for helpful discussions. The data from Experiment 1 were presented at a meeting of ARVO (Chase *et al.,* 1993).